 https://doi.org/10.3311/PPci.14472

Periodica Polytechnica Civil Engineering, 64(4), pp. 1064–1074, 2020

Centrifuge Modelling and Finite Element Analysis of Laterally Loaded Single Piles in Sand with Focus on *P–Y* Curves

Hocine Haouari[1*], Ali Bouafia[1]

[1] Department of Civil Engineering, Faculty of Technology, University of Blida, P.O. Box 270, R. P Blida 09000, Algeria
[*] Corresponding author, e-mail: haouari.hocine@etu.univ-blida.dz

Received: 09 June 2019, Accepted: 05 July 2020, Published online: 11 August 2020

Abstract

Centrifuge modelling and finite element analysis are powerful tools of research on the lateral pile/soil interaction. This paper aims at presenting the main results of experimental and numerical analysis of the pile response under monotonic lateral loading in sand. After description of the experimental devices, it focuses on the determination of the load-transfer *P-Y* curves for rigid and semi-rigid piles embedded in dry dense sand by using the experimental bending moment profiles obtained in centrifuge tests, as well as by a three-dimensional finite element models using ABAQUS Software. The elastic perfectly plastic Mohr-Coulomb constitutive model has been used to describe the soil response, and the surface-to-surface contact method of ABAQUS software has been used to take into account the nonlinear response at soil/pile interface. The analysis methodology has allowed to propose a hyperbolic function as a model to construct P-Y curves for rigid and semi-rigid piles embedded in dry dense sand, this model is governed by two main parameters, which are the initial subgrade reaction modulus, and the lateral soil resistance, the latter has been formulated in terms of Rankine's passive earth pressure coefficient, the sand dry unit weight, and the pile diameter.

Keywords

pile, lateral load, centrifuge modelling, finite element modelling, P-Y curves, initial subgrade reaction modulus, lateral soil resistance

1 Introduction

Pile foundations are often laterally loaded due to many sources such as wind, traffic and earthquakes. Lateral loading of the piles occurs either in active form as concentrated loads at the pile head, or passively as distributed pressure acting by the soil along the pile shaft. Horizontal loading sometimes becomes as a key parameter for the design of pile foundations, such in case of monopile foundations of offshore wind turbines, which are subjected to very important lateral loads such as, wind and wave loads.

Several design methods have been proposed in the literature but most of them are based on simplistic mechanisms of pile/soil interaction. Although the full-scale lateral loading test is a pragmatic approach to predict the pile response, its relatively high cost eclipses its field of application to relatively important projects. However, physical and numerical modelling are an important alternative to such approaches and are widely used in engineering practice as well as in research.

The problem of laterally loaded piles has been analyzed in the literature using different approaches which may be subdivided into four main categories, namely: the elastic continuum models where the soil is represented by a linear elastic continuum [1, 2] which have the advantage of taking into account the continuity of the soil material, but they are limited to small deformations behavior.

The second category encompasses the numerical methods. In fact, important advances in the field of computer science these last decades allows developing powerful numerical methods which are widely used for the analysis of piles under lateral loads, such as the finite element method and the finite difference one [3, 5], these methods offer the advantage of taking into account the material nonlinearity of the soil/pile system, through increasingly developed constitutive models.

The third one contains the semi-empirical or empirical methods [6, 7], while the last category is called the subgrade reaction methods (called also the *P-Y* curves methods),

Cite this article as: Haouari, H., Bouafia, A. "Centrifuge Modelling and Finite Element Analysis of Laterally Loaded Single Piles in Sand with Focus on P-Y Curves", Periodica Polytechnica Civil Engineering, 64(4), pp. 1064–1074, 2020. https://doi.org/10.3311/PPci.14472

which are based on the model of beam on elastic foundations suggested first by Winkler [8]. First generation of the *P-Y* curves method was developed by Matlock [9] and Reese et al. [10], and subsequently adopted by the API [11].

The pile is modelled by a linear elastic beam surrounded by a series of infinite independent nonlinear springs characterized by the subgrade reaction modulus E_s, as illustrated in Fig. 1. The pile bending is then governed by a fourth order nonlinear differential equation, the term E_pI_p being the pile flexural stiffness:

$$E_pI_p\frac{d^4Y}{dz^4}+E_sY=0. \quad (1)$$

Most of the proposed methods for the construction of the *P-Y* curves are empirical and based on lateral loading tests of full-scale piles [9–15], while the other ones are semi-empirical and based on the analogy of the soil reaction with the pressuremeter test [16–18].

Physical modelling using the geotechnical centrifuge is a powerful tool not only for the development of *P-Y* curves but also for conducting parametric studies to evaluate the effect of different parameters on the response of piles under lateral loading [19–22]. Table 1 summarizes the main similarity scales used within the scope of the topic, the similarity scale X^* of a parameter X being the ratio of the X_{model} to $X_{prototype}$. L^* is then the dimension scale of the physical model.

The purpose of this paper is to present the main results of physical modelling in centrifuge, as well as numerical analysis based on 3D finite element model using ABAQUS Software, of a single pile response under monotonic lateral loading in sand. Focus is made on the determination of the *P-Y* curves for two piles: semi-rigid pile denoted hereafter P_1 and having slenderness ratio of 10, and a rigid pile denoted P_2 and having slenderness ratio of 5.55, both of the piles being embedded in dry dense sand.

From the results found, a model has been proposed for the construction of *P-Y* curves for rigid, and semi-rigid piles embedded in dry dense sand, this model depends essentially on the initial subgrade reaction modulus, and the lateral soil resistance.

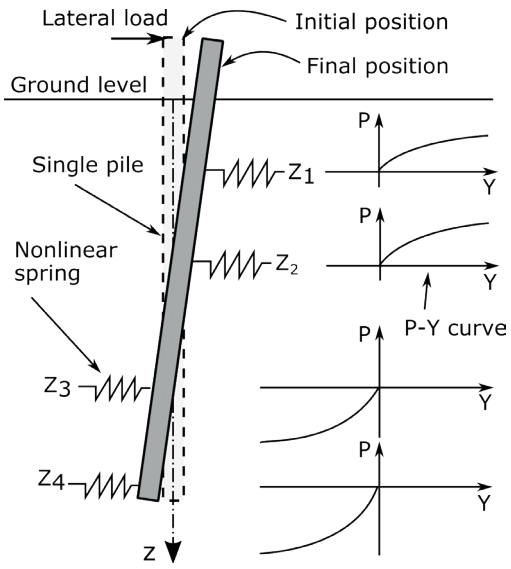

Fig. 1 General scheme of the *P-Y* curves method

Table 1 Summary of the main similarity scales

Parameter X	Scale X^*
Terrestrial gravity acceleration	$(L^*)^{-1}$
Stress	1
Strain	1
Displacement	L^*
Force	$(L^*)^2$
Bending Moment	$(L^*)^3$
Flexural stiffness	$(L^*)^4$
Elasticity modulus	1
Poisson's ratio	1
Friction angle	1
Cohesion	1

2 Centrifuge modelling

2.1 Description of the centrifuge

Lateral loading tests on small scale models were carried out by Bouafia [23] in the geotechnical centrifuge of the IFSTTAR (Formerly LCPC) in France which is a powerful device of physical modelling characterized by a radius of 5.5 m, a maximum mass of rotating model of 2000 kg and a maximum centrifuge acceleration of 200 times the terrestrial gravity acceleration g (g = 10 m/s^2). Fig. 2 illustrates the geotechnical centrifuge of the IFSTTAR.

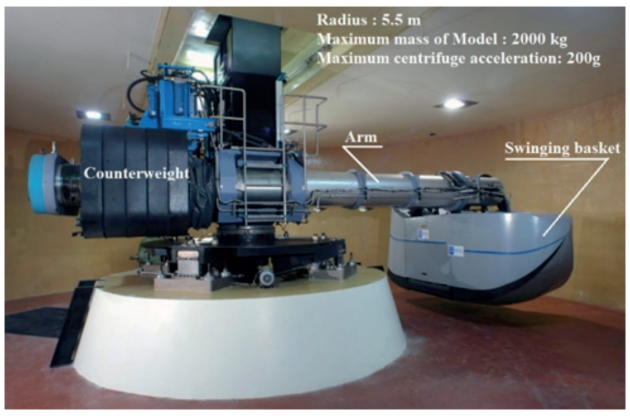

Fig. 2 Geotechnical centrifuge of the IFSTTAR

2.2 Description of the pile models

The pile models are tubes made of Duralumin AU-4G, these models have been instrumented by 12 equidistant pairs of strain gauges along two diametrically opposite axes, and two displacement transducers (LVDT) placed on the pile top, as depicted in Fig. 3. Table 2 summarizes the main properties of the two piles studied in geotechnical centrifuge.

The installation of pile models has been carried out at 1 g, i. e. before placing the container in the centrifuge and starting the centrifugation. The pile models have been installed into the sand by manual jacking at low rate. In order to get rough surfaces of the models, the sand was glued at their shafts.

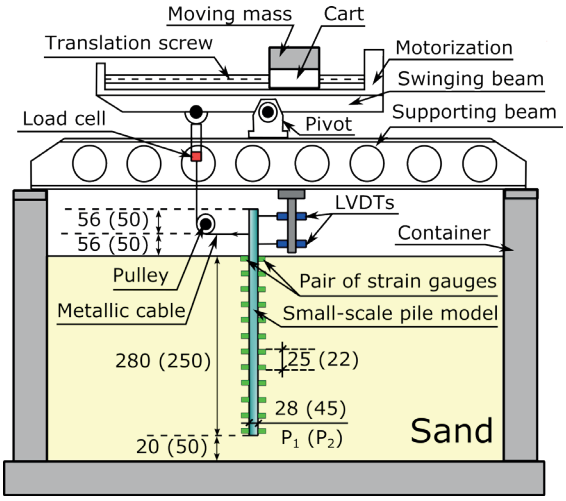

Fig. 3 Schematic of testing arrangement, dimensions are in mm, dimensions between brackets are for pile P_2

Table 2 Main geometrical and mechanical properties of piles

	Pile P_1		Pile P_2	
	Prototype	Model	Prototype	Model
Scale	1	1/17.85	1	1/20
Outside diameter B (mm)	500	28.07	900	45.02
Inside Diameter (mm)	456.60	25.58	810.4	40.52
Pile length L (mm)	7000	392	7000	350
Embedded length D (mm)	5000	280	5000	250
Pile length above the ground surface (mm)	2000	112	2000	100
Spot height of lateral load (mm)	1000	56	1000	50
Slenderness ration D/B	10	10	5.55	5.55
Flexural stiffness E_pI_p (Nm^2)	56.65 10^6	558	740.9 10^6	4631
Limit elastic stress σ_e (MPa)	171	171	260	260

Lateral loads were applied up to 200 kN for pile P_1 and up to 483.5 kN for pile P_2, by increments of 3 minutes of duration by a loading device, the latter is illustrated in Fig. 4, and schematized in Fig. 3, Where a beam swings around a pivot due to a moving mass, which generates tension in a metallic cable, the latter is attached to the pile head, which causes lateral displacement of the pile. Remote control of the mass movement allows assigning a well-controlled load increments program to the model, which is the main advantage of this experimental device [24].

Centrifuge acceleration corresponds to the inverse of the dimension scale L^*, that is to say 17.85 times the terrestrial gravity acceleration for pile P_1, and 20 times for pile P_2.

2.3 Description of the soil model

The soil used is clean dry red quartzite poorly graded sand from Le-Rheu site (Rennes, France) classified as an SP sand according to the USCS system. Its dry unit weight γ_d is 16.5 kN/m^3 corresponding to a density index I_D of 92 % (very dense sand), and the measured internal friction angle by a direct shear test is 42°.

Static cone penetration tests (CPT) with a miniature penetrometer were carried out during the centrifugation, just before the start of the loading tests. The rod length of this penetrometer is 200 mm, its cone diameter is of 6 mm. Load cell and LVDT transducer are fixed on the cone in order to measure continuously the cone resistance q_c at various depths.

Fig. 5 represents a typical penetration resistance profile obtained at centrifuge acceleration of 20 g, g being the gravitational acceleration.

It is to be noticed that the cone resistance profiles are hyperbolic shaped, and may be fitted by the following equation:

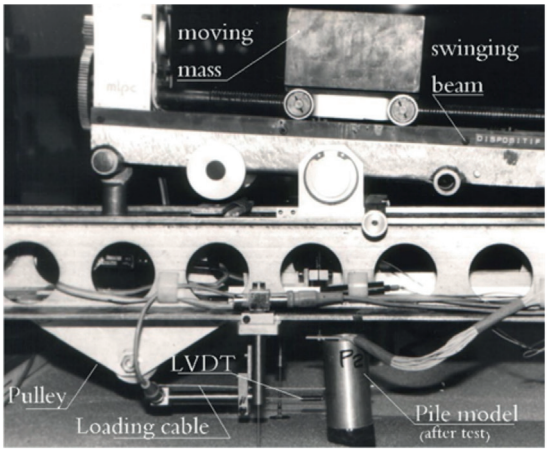

Fig. 4 Loading device of pile models

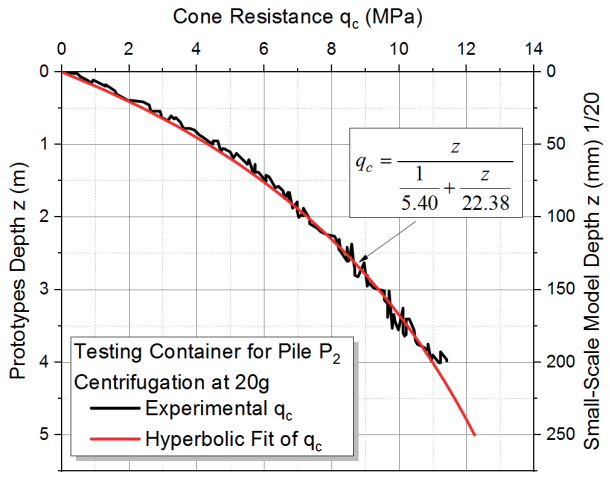

Fig. 5 Cone resistance profile in testing container for pile P_2

$$q_c = \frac{z}{\frac{1}{E_c} + \frac{z}{q_{cu}}}, \tag{2}$$

where E_c and q_{cu} are respectively called the shallow cone stiffness and the deep cone resistance.

In geotechnical literature, there are several correlations between the sand elastic modulus E and the cone resistance q_c and the ratio E/q_c is ranging between 2.5 and 3.5 [25].

Elastic sand modulus E was estimated from the cone resistance q_c by multiplying it by an average factor of 3 as shown in the Eq. (3) and was then assumed increasing with depth following a hyperbolic function.

$$E = 3q_c \tag{3}$$

The results presented hereafter correspond to the prototype scale of a rough pile installed by jacking into a very dense dry sand.

2.4 Construction of *P-Y* curves

Measurements obtained for each lateral load increment are the top lateral displacements, and the axial deformations $\varepsilon(z)$ along the pile shaft by means of strain gauges, which allow calculating the experimental bending moment $M(z)$ as follows:

$$M(z) = 2E_p I_p \frac{\varepsilon(z)}{B}. \tag{4}$$

The *P-Y* curves describe the relationship between the soil lateral reaction P and the pile lateral displacement Y. In most cases, they are derived from the experimental bending moment profile $M(z)$.

The deformations are measured at strain gauges levels, therefore the resulting experimental bending moment profile consist of discrete points that form a broken line, it is convenient to fit the latter by a continuous function.

Several methods have been used to fit experimental bending moment profiles, among these methods, we find smoothing by cubic and quintic splines [24, 26], polynomial fitting [27, 28], and the weighted residual method [27].

In this study, we fitted the experimental bending moment profiles by single term Fourier series using MATLAB software [29], with a fitting coefficient of 98 %, Eq. (5) describes Fourier series form used herein.

$$M(z) = a_0 + a_1 \cos(\omega z) + b_1 \sin(\omega z), \tag{5}$$

where a_0, a_1, b_1, and ω are coefficients of the Fourier series.

The profile thus found is differentiated twice to obtain the soil lateral reaction P as given by Eq. (6) and integrated twice to obtain the pile lateral displacement Y as shown by Eq. (7). The integration constants are calculated from the displacement measurements on the pile head. Figs. 6 and 7 illustrate the soil lateral reaction P, and the pile lateral displacement for pile P_1 and P_2, respectively.

$$P = -\frac{d^2 M}{dz^2} \tag{6}$$

$$Y = \frac{1}{E_p I_p} \iint M \, dz \, dz + Y_0' z + Y_0 \tag{7}$$

Based on soil lateral reaction P, and pile lateral displacement Y, we plotted *P-Y* curves for piles P_1 and P_2 as shown in Fig. 8 and Fig. 9. We plotted these curves for the same depths where we plotted the ABAQUS FEM *P-Y* curves.

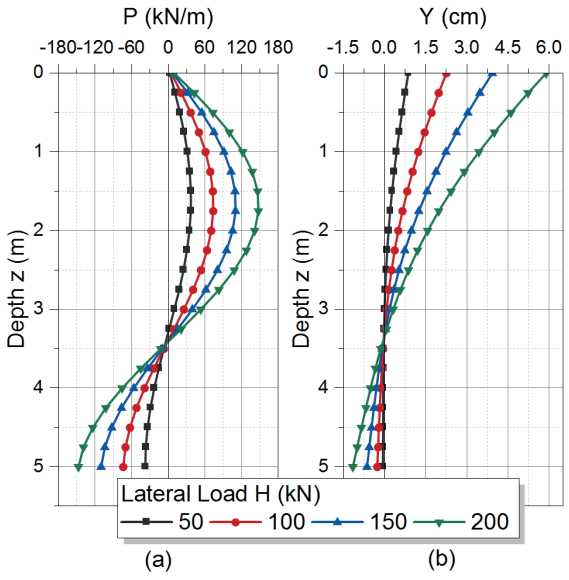

Fig. 6 Pile P_1, (a) Experimental soil lateral reaction, (b) Experimental pile lateral displacement

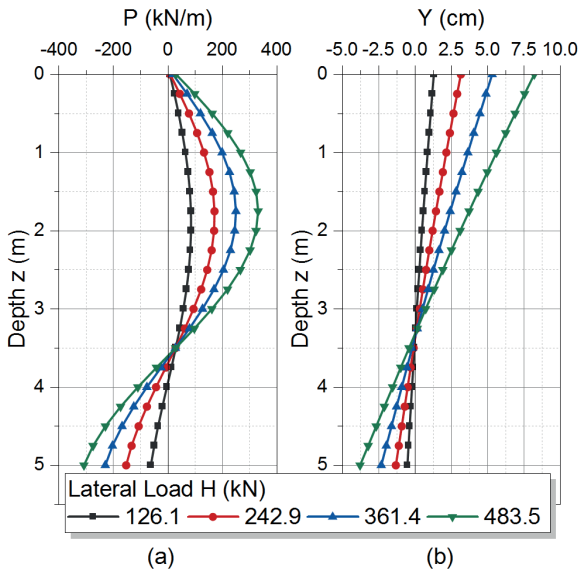

Fig. 7 Pile P_2, (a) Experimental soil lateral reaction, (b) Experimental pile lateral displacement

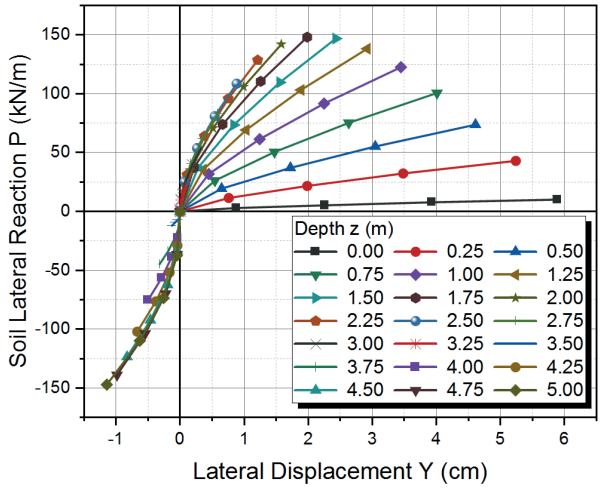

Fig. 8 Set of Experimental *P-Y* curves for pile P_1

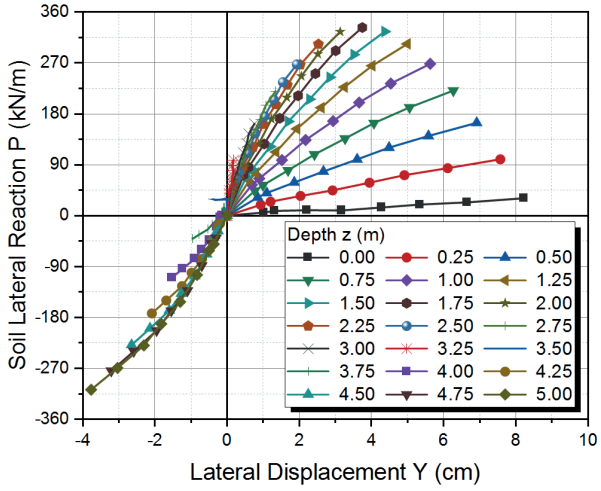

Fig. 9 Set of Experimental *P-Y* curves for pile P_2

By observing these *P-Y* curves, it can be noticed an inherent nonlinearity even at small displacements. Moreover, for a given load, the lateral soil stiffness which may be quantified by the secant slope of *P-Y* curves increases with depth. It will be shown hereafter a linear variation of lateral soil stiffness versus depth which is typical of a Gibson's soil.

Given their shapes, the *P-Y* curves may be well fitted by the following hyperbolic function:

$$P = \frac{Y}{\frac{1}{E_{ti}} + \frac{Y}{P_u}}, \tag{8}$$

where E_{ti} is the initial subgrade reaction modulus, describing a linear relationship between the soil lateral reaction P and the pile lateral displacement Y for small deformations, as shown by Eq. (9).

$$E_{ti} = \frac{P}{Y} \tag{9}$$

Fig. 10 shows that this modulus increases linearly with the depth z, with a gradient (slope) denoted N_h, as indicated by Eq. (10).

$$E_{ti} = N_h z \tag{10}$$

Moreover, the values of this gradient are very close for both piles, in spite of the large differences in slenderness ratio (D/B), and in diameter as mentioned in Table 2. The average experimental gradient equals 9 MN/m^3.

P_u is the lateral soil resistance corresponding to large pile displacements. It is the horizontal asymptote of the *P-Y* curve, which corresponds to the maximum mobilized soil lateral reaction.

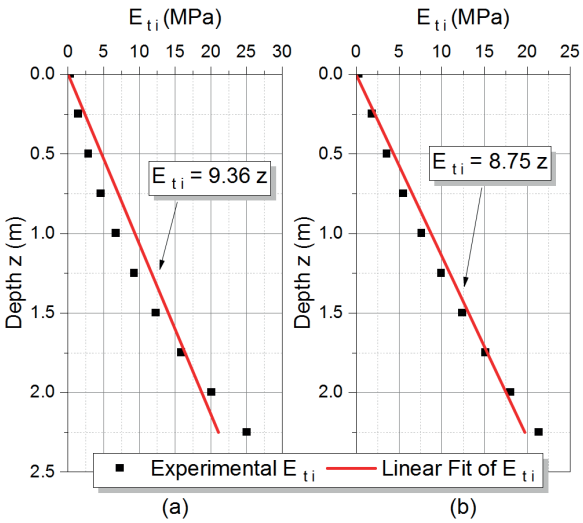

Fig. 10 Experimental profile of E_{ti}, (a) pile P_1, (b) pile P_2

Fig. 11 illustrates the normalized lateral resistance $P_u/(\gamma_d zB)$ against the normalized depth z/B, the normalized lateral resistance decreases gradually until it vanishes at a depth equivalent to 6.75 B for Pile P_1, and 3.75 B for pile P_2, which corresponds to about 0.7 D. The normalized lateral resistances become negative below these depths.

3 Finite Element Modelling

The prototype piles P_1 and P_2 are simulated by three-dimensional finite element models using ABAQUS software [30]. Due to the symmetry with respect to the plane defined by the lateral loading line and the neutral axis of the pile, it was simulated only half the pile/soil system.

As depicted by Fig. 12, finite element models have a semi-cylindrical shape and encompass two parts which are the tubular pile and the surrounding soil. The FEM model height is 10 m (2 D) and its radius is 15 m (3 D), these dimensions have been adopted in such a way that the boundaries do not affect the results. The mesh is regular and symmetric to the neutral axis of the pile, it is also more refined in the vicinity of the pile because there is a concentration of stresses in this zone.

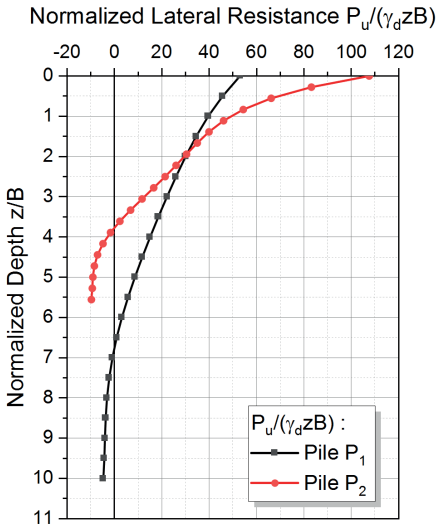

Fig. 11 Experimental normalized profiles of P_u

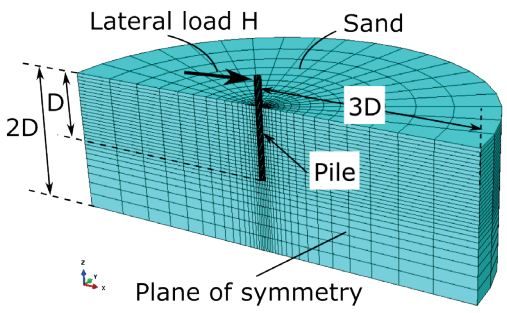

Fig. 12 Three-dimensional finite element model

Mohr-Coulomb elastic-perfectly plastic constitutive model was used to describe the soil response and the representative parameters are summarized in Table 3. Pile material is however assumed to be linear elastic.

The surface-to-surface contact method of ABAQUS software has been used to take into account the nonlinear response at soil/pile interface.

The tubular pile are represented by 4-node, quadrilateral, stress-displacement shell elements with reduced integration and a large-strain formulation "S4R", while the soil is modelled by three-dimensional continuum stress/displacement, 8-node, reduced integration elements "C3D8R" [30].

The plane of symmetry is fixed against any displacements in the y direction, the back surface is fixed against displacements in the x and y directions, and of course the base of the model is fixed against displacements in all directions.

Considering the hyperbolic increase of the elastic modulus E with the depth z, the sand material is defined in ABAQUS through the "user-defined field" option. First a "field variable" as depth z is added through the Material Editor of ABAQUS/CAE, and then it was written a user-defined filed USDFLD subroutine in FORTRAN Language within the Microsoft Visual Studio environment. This subroutine, defining the hyperbolic variation of elastic modulus E with vertical coordinates, was incorporated to ABAQUS through the Job Editor, and finally the compilation and calculation were carried out with Intel FORTRAN Compiler.

The interfacial friction between the pile and the sand was taken into account according to the "contact pairs" (surface to surface) approach of ABAQUS using the "basic Coulomb friction model" which assumes that the friction coefficient μ is the same in all directions (isotropic friction). It was adopted a value of 1.0 for μ, i.e. an interfacial friction angle δ equal to the sand internal friction angle φ due to the roughness of pile/soil interface.

Table 3 Parameters of Mohr-Coulomb law for sand

Parameter	Sand for P_1	Sand for P_2
Dry unit weight γ_d (kN/m^3)	16.5	16.5
Internal friction angle φ (deg)	42	42
Dilation angle ψ (deg)	12	12
Cohesion C (kPa)	0.05	0.05
Poisson's ratio v_s	0.3	0.3
Shallow cone stiffness E_c (MN/m^3)	5.07	5.40
Deep cone resistance q_{cu} (MPa)	20.88	22.38

The analysis is performed in two steps; the first is a "geostatic" step that is used to reproduce the initial stress condition in the soil by applying its dry self-weight as "body force", the second step is a "general static" step in which the lateral load H is applied to the pile head as a "concentrated load".

4 Validation of Finite Element Model

The comparison is focused on the load-displacement curves at ground surface and the bending moment profiles along the pile shaft. Fig. 13 shows the load-displacement curves of Pile P_1 and Pile P_2, obtained from centrifuged model tests and the three-dimensional finite element models. It may be noticed that load-displacement curves derived from physical centrifuge modelling are fairly close to those developed from numerical finite element modelling, especially for very small displacements.

Fig. 14 illustrates the bending moment profiles, where it can be seen that differences between experimental and numerical profiles are very small. Based on these observations, especially those for bending moment profiles, we consider that the results are sufficiently coherent to say that the ABAQUS finite element models are valid.

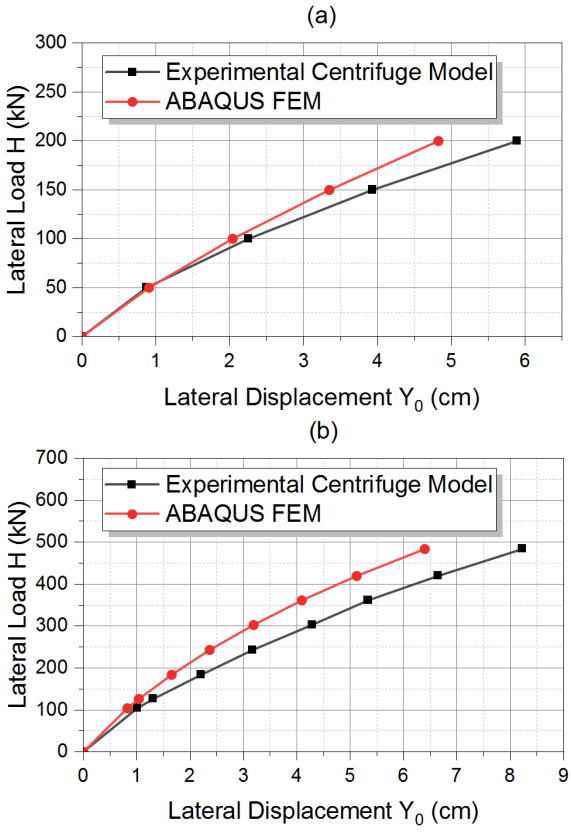

Fig. 13 Load-Displacement curve at the ground surface, (a) for pile P_1, (b) for pile P_2

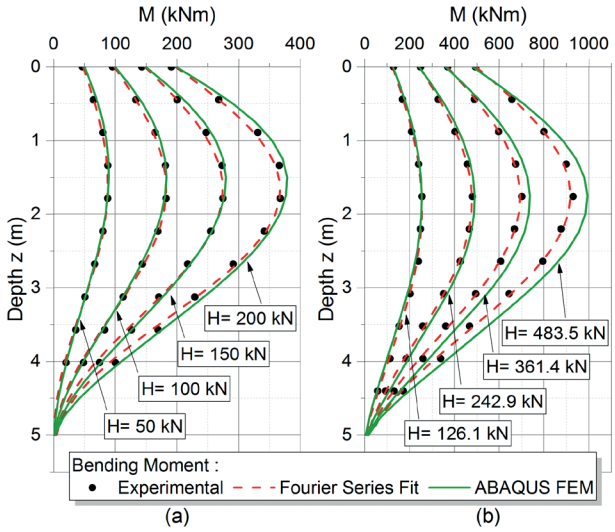

Fig. 14 Bending moment profiles, (a) pile P_1 (b) Pile P_2

5 Determination of *P-Y* curves

From the "job results" option of ABAQUS, the lateral displacement Y and the rotation Y' along the pile shaft were directly collected through the "ODB field output" option, while the shear force T and bending moment M were obtained by specifying all "elements and nodes" cross-sections of the pile using the "Free Body Cut" option, then extracted by means of the "Free Body" output option. The first derivative of the shear force T yields the lateral reaction P of the soil as indicated by the Eq. (11). Knowing the profiles of P and Y, it is possible to construct the P-Y curves derived from the three-dimensional finite element models.

$$P = -\frac{dT}{dz} \tag{11}$$

Fig. 15(b) shows the lateral displacement profile of the pile P_1, exhibiting some flexibility expressed by a certain curvature which characterizes the semi-rigid pile deformability. The center of rotation (point of zero displacement) is located at about 0.75 D. Fig. 16(b) shows the lateral displacement of the pile P_2, where the deformed shape is a rather straight line which characterizes the rigid pile deformability, the centrer of rotation being located at about 0.8 D.

Figs. 15(a) and 16(a) illustrate the profiles of soil lateral reaction for piles P_1 and P_2, respectively, where it can be seen that the center of pressure (point of zero soil reaction) coincide with the center of rotation, confirming the fundamental postulate of Winkler according to which P is proportional to Y and have therefore both the same sign.

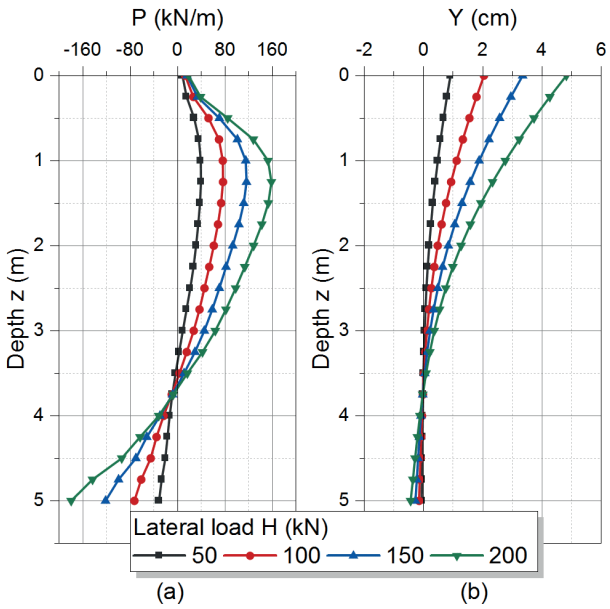

Fig. 15 Pile P_1, (a) FEM soil lateral reaction, (b) FEM pile lateral displacement

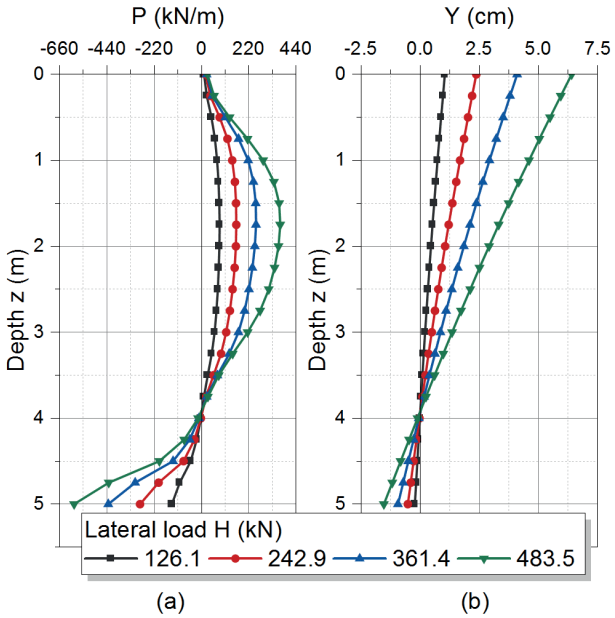

Fig. 16 Pile P_2, (a) FEM soil lateral reaction, (b) FEM pile lateral displacement

Figs. 17 and 18 show *P-Y* curves for pile P_1 and P_2 respectively. Following the same methodology of interpretation of the experimental *P-Y* curves described in Section 2.4, the initial subgrade reaction modulus E_{ti} and the lateral soil resistance P_u was derived.

In Fig. 19 are illustrated the profiles of E_{ti} for piles P_1 and P_2 which exhibit a remarkable linear variation along the pile which is typical to Gibson's soil model characterized by a linear stiffness profile. From Fig. 19 and Fig. 10, it may be noticed that experimental and the FEM gradients

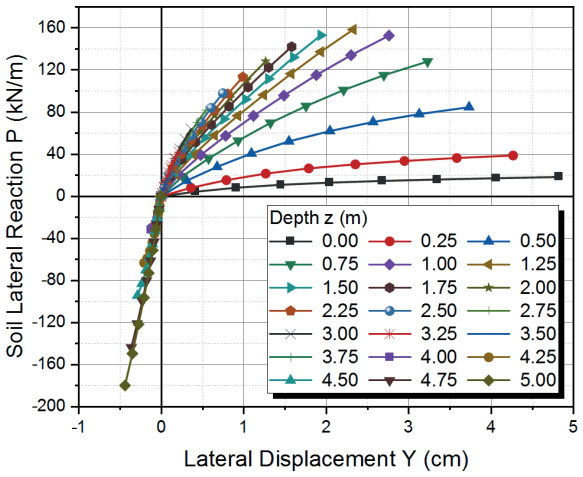

Fig. 17 Set of FEM *P-Y* curves for pile P_1

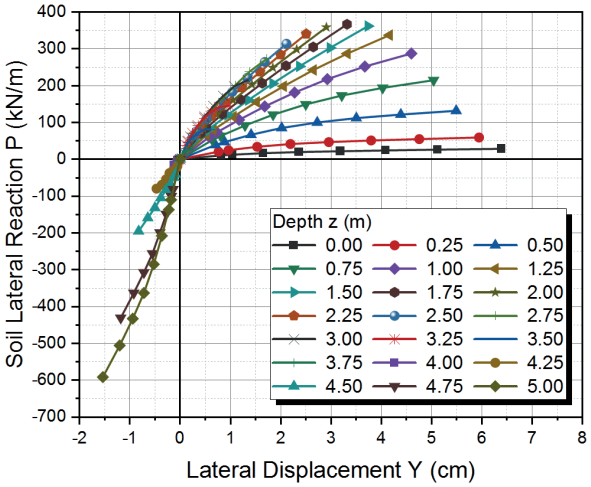

Fig. 18 Set of FEM *P-Y* curves for pile P_2

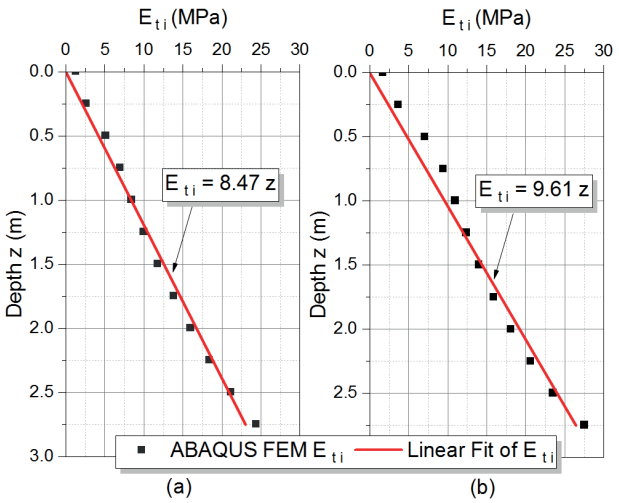

Fig. 19 FEM profile of E_{ti}, (a) pile P_1, (b) pile P_2

N_h are comparatively close, moreover the average numerical gradient is equal to 9 MN/m^3, i.e. equal to the average experimental gradient.

The calculated values of the gradient N_h are within the range of values proposed by Terzaghi [31] for the same sand density as shown in the Table 4, then the method of the latter can be used to calculate the gradient N_h, and thus to estimate the initial subgrade reaction modulus E_{ti}.

Figs. 20 and 21 illustrate the profiles of lateral soil resistance P_u for pile P_1 and P_2, respectively, given their triphasic forms, we fitted them by piecewise linear functions with three segments PWL3 using OriginPro software [32]. Subsequently, each segment was formulated in terms of the Rankine's passive earth pressure coefficient K_p, the dry unite weight γ_d, and the pile diameter B as indicated by Eq. (13).

$$K_p = \tan^2(45 + \varphi/2), \tag{12}$$

$$P_u = aK_p^2\gamma_d B(z+b), \tag{13}$$

where a and b are the coefficients of lateral soil resistance P_u, these coefficients are summarized in Table 5. It is assumed that the formulae obtained for the pile P_1 are valid for the semi-rigid piles, and those suggested for the pile P_2 are valid for rigid piles. Fig. 22 illustrates the typical P-Y curve proposed herein.

Table 4 Gradient N_h according to Terzaghi (1955)

Dry unite weight γ_d (kN/m³)	13–15	15–17	17–19
N_h (MN/m³)	0.96–3.30	3.30–12.60	12.60–28.10

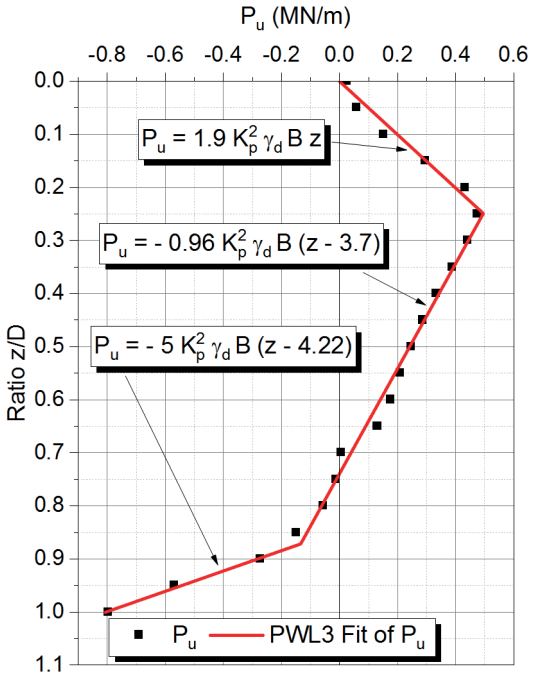

Fig. 20 Lateral soil resistance for semi-rigid piles

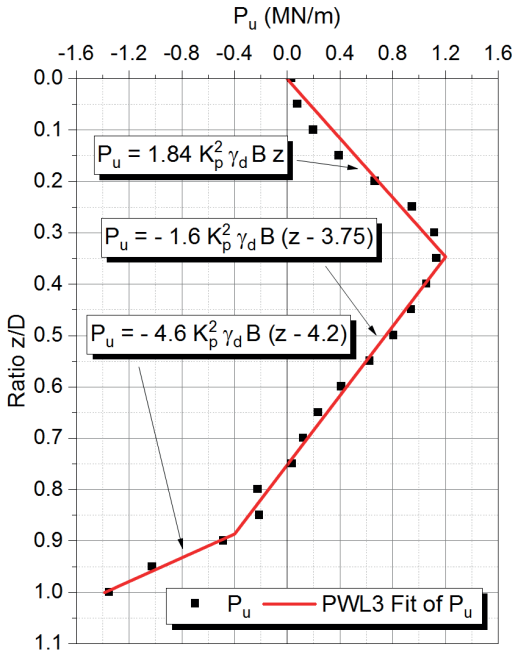

Fig. 21 Lateral soil resistance for rigid piles

Table 5 Coefficients of lateral soil resistance

Type of pile	Pile intervals	P_u coefficients	
		a	b
Semi-rigid piles	0 - 0.25D	1.90	0.00
	0.25D - 0.87D	-0.96	-3.70
	0.87D - D	-5.00	-4.22
Rigid piles	0 - 0.35D	1.84	0.00
	0.35D - 0.90D	-1.60	-3.75
	0.90D - D	-4.60	-4.20

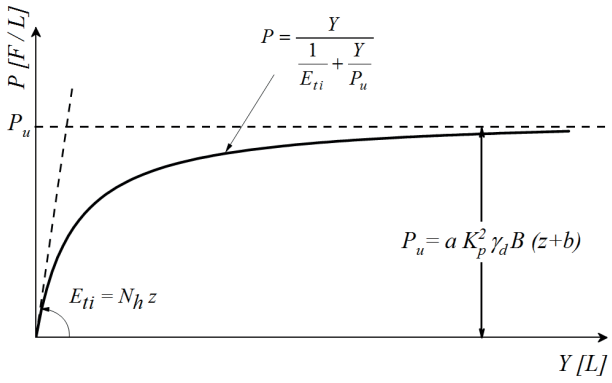

Fig. 22 Typical P-Y curve proposed

6 Conclusions

In this paper were presented and analyzed the main results of experimental and numerical modelling of the load-deflection behavior of two piles under monotonic lateral loading in dense sand. Brief description of the experimental devices used in centrifuge tests was followed by the presentation of the methodology of construction of the

experimental *P-Y* curves and the determination of initial subgrade reaction modulus E_{ti}, as well as the lateral soil resistance P_u.

It was found that E_{ti} is almost independent of the slenderness ratio *D*/*B*, and also of pile diameter *B*. Moreover, normalized lateral soil resistance was found decreasing with depth and vanishing at about 0.7 of the pile embedded length *D*.

The second part of the paper was devoted to a three-dimensional finite element modelling using ABAQUS Software. The nonlinear response of the sand was described by elastic perfectly plastic Mohr-Coulomb constitutive model, where the elastic soil modulus was estimated by correlation with the static cone penetration resistance. Soil modulus was assumed increasing with depth following a hyperbolic function and was implemented in ABAQUS through the USDFLD user subroutine. The FEM model was validated by comparing the results with those of the centrifuged model which showed quite good coherence in terms of load-deflection curves, as well as the bending moment profiles.

Pile lateral displacements and soil lateral reaction along the pile shaft were derived through the "free body" option of ABAQUS, and the *P-Y* curves were constructed for each given depth *z*. The parameters of the *P-Y* curves were obtained by hyperbolic fitting of the *P-Y* curves. It was found that both experimental and numerical E_{ti} moduli have a linear variation with depth, confirming the Gibson's soil model for homogeneous cohesionless soils. Terzaghi method [31] may be used to estimate the initial subgrade reaction modulus E_{ti}.

Analysis of the lateral soil resistance P_u led to a preliminary recommendation to estimate it for semi-rigid, and rigid piles embedded in dense sand, we formulated the lateral soil resistance P_u through a trilinear function, which depends on the Rankine's passive earth pressure coefficient K_p, the sand dry unit weight γ_d, and the pile diameter *B*.

Subsequent work will focus on a thorough detailed comparative study with current design methods available in literature.

References

[1] Poulos, H. G. "Behavior of Laterally Loaded Piles: I-Single Piles", Journal of the Soil Mechanics and Foundations Division, 97(5), pp. 711–731, 1971.

[2] Budhu, M., Davies, T. G. "Nonlinear analysis of laterality loaded piles in cohesionless soils", Canadian Geotechnical Journal, 24(2), pp. 289–296, 1987. https://doi.org/10.1139/t87-034

[3] Brown, D. A., Shie, C.-F. "Three dimensional finite element model of laterally loaded piles", Computers and Geotechnics, 10(1), pp. 59–79, 1990. https://doi.org/10.1016/0266-352X(90)90008-J

[4] Ng, C. W. W., Zhang, L. M. "Three-Dimensional Analysis of Performance of Laterally Loaded Sleeved Piles in Sloping Ground", Journal of Geotechnical and Geoenvironmental Engineering, 127(6), pp. 499–509, 2001. https://doi.org/10.1061/(ASCE)1090-0241(2001)127:6(499)

[5] Szepesházi, A., Mahler, A., Móczár, B. "Three Dimensional Finite Element Analysis of Deep Excavations' Concave Corners", Periodica Polytechnica Civil Engineering, 60(3), pp. 371–378, 2016. https://doi.org/10.3311/PPci.8608

[6] Brettmann, T., Duncan, J. M. "Computer Application of CLM Lateral Load Analysis to Piles and Drilled Shafts", Journal of Geotechnical Engineering, 122(6), pp. 496–498, 1996. https://doi.org/10.1061/(ASCE)0733-9410(1996)122:6(496)

[7] Briaud, J.-L. "SALLOP: Simple Approach for Lateral Loads on Piles", Journal of Geotechnical and Geoenvironmental Engineering, 123(10), pp. 958–964, 1997. https://doi.org/10.1061/(ASCE)1090-0241(1997)123:10(958)

[8] Winkler, E. "Die Lehre von der Elasticitaet und Festigkeit" (The theory of elasticity and strength), Dominicus, Prague, Czechoslovakia, 1867. (in German)

[9] Matlock, H. "Correlations for Design of Laterally Loaded Piles in Soft Clay", In: Offshore Technology Conference, Houston, TX, USA, 1970, pp. 577–594. https://doi.org/10.4043/1204-ms

[10] Reese, L. C., Cox, W. R., Koop, F. D. "Analysis of Laterally Loaded Piles in Sand", In: Offshore Technology Conference, Houston, TX, USA, 1974, pp. 473–483. https://doi.org/10.4043/2080-MS

[11] API "API RP 2A-WSD Recommended Practice for Planning, Designing and Constructing Fixed Offshore Platform - Working Stress Design", American Petroleum Institute, Washington, DC, USA, 2000.

[12] Reese, L. C., Welch, R. C. "Lateral Loading of Deep Foundations in Stiff Clay", Journal of the Geotechnical Engineering Division, 101(7), pp. 633–649, 1975.

[13] O'Neill, M. W., Reese, L. C., Cox, W. R. "Soil Behavior for Piles Under Lateral Loading", In: Offshore Technology Conference, Houston, TX, USA, 1990, pp. 279–287. https://doi.org/10.4043/6377-MS

[14] Bouafia, A. "Single piles under horizontal loads in sand: determination of P–Y curves from the prebored pressuremeter test", Geotechnical and Geological Engineering, 25, pp. 283–301, 2007. https://doi.org/10.1007/s10706-006-9110-7

[15] Bouafia, A. "Laterally loaded single piles - Construction of P-Y curves from the cone penetration test", In: Proceedings of the 19th International Conference on Soil Mechanics and Geotechnical Engineering, ICSMGE, Seoul, South Korea, 2017, pp. 2957–2960. [online] Available at: https://www.issmge.org/uploads/publications/1/45/06-technical-committee-20-tc214-04.pdf

[16] Briaud, J. L., Smith, T. O., Meyer, B. J. "Using the Pressuremeter Curve to Design Laterally Loaded Piles", In: Offshore Technology Conference, Houston, TX, USA, 1983, pp. 495–502. https://doi.org/10.4043/4501-MS

[17] Ménard, L., Bourdon, G., Gambin, M. "Méthode générale de calcul d'un rideau ou d'un pieu sollicité horizontalement en fonction des résultats pressiomètriques", Journal Sols Soils, 22/23(6), pp. 16–29, 1971. (in French)

[18] Narimani, S., Chakeri, H., Davarpanah, S. M. "Simple and Non-Linear Regression Techniques Used in Sandy-Clayey Soils to Predict the Pressuremeter Modulus and Limit Pressure: A Case Study of Tabriz Subway", Periodica Polytechnica Civil Engineering, 62(3), pp. 825–839, 2018. https://doi.org/10.3311/PPci.12063

[19] Georgiadis, M., Anagnostopoulos, C., Saflekou, S. "Centrifugal testing of laterally loaded piles in sand", Canadian Geotechnical Journal, 29(2), pp. 208–216, 1992. https://doi.org/10.1139/t92-024

[20] Bouafia, A., Garnier, J. "Experimental study of p–y curves for piles in sand", In: Proceedings of the International Conference Centrifuge 1991, Boulder, CO, USA, 1991, pp. 261–268.

[21] Lyndon, A., Pearson, R. A. "Skin friction effects on laterally loaded large diameter piles in sand", In: Proceedings of the International Conference on Geotechnical Centrifuge Modelling, Paris, France, 1988, pp. 363–370.

[22] Farkas, D., Hajnal, G., Vasvári, V. "Validation of a Physical and Numerical Model to Solve Problems of Seepage Flow", Periodica Polytechnica Civil Engineering, 63(2), pp. 388–400, 2019. https://doi.org/10.3311/PPci.12592

[23] Bouafia, A. "Modélisation des pieux chargés latéralement en centrifugeuse" (Centrifuge modelling of laterallyloaded piles), PhD Thesis, University of Nantes, 1990. (in French)

[24] Bouafia, A. "Horizontal loading of piles-Comparative study of P-Y curves-based methods", In: 3rd International Symposium on Deformation Characteristics of Geomaterials, IS LYON 2003, Lyon, France, 2003, pp. 897–903.

[25] Bouafia, A. "Génie Civil Conception et Calcul des Ouvrages Geotechniques" (Civil engineering: design and analysis of geotechnical structures), Pages Bleues, Algiers, Algeria, 20011. (in French)

[26] Mezazigh, S., Levacher, D. "Laterally loaded piles in sand: slope effect on P-Y reaction curves", Canadian Geotechnical Journal, 35(3), pp. 433–441, 1998. https://doi.org/10.1139/t98-016

[27] Wilson, D. W. "Soil-Pile-Superstructure Interaction in Liquefying Sand and Soft Clay", PhD Dissertation, University of California, 1998. [online] Available at: https://ucdavis.app.box.com/s/8qd4nx3gspt2dnp74oev

[28] Ilyas, T., Leung, C. F., Chow, Y. K., Budi, S. S. "Centrifuge Model Study of Laterally Loaded Pile Groups in Clay", Journal of Geotechnical and Geoenvironmental Engineering, 130(3), pp. 274–283, 2004. https://doi.org/10.1061/(ASCE)1090-0241(2004)130:3(274)

[29] MathWorks "MATLAB (R2019b) Documentation" [computer program] Available at: https://fr.mathworks.com/help/matlab/index.html

[30] Dassault Systèmes Simulia "ABAQUS 2016 Documentation", [computer program] Available at: http://130.149.89.49:2080/v2016/index.html

[31] Terzaghi, K. "Evaluation of Coefficients of Subgrade Reaction", Géotechnique, 5(4), pp. 297–326, 1955. https://doi.org/10.1680/geot.1955.5.4.297

[32] OriginLab "OriginPro (2019) Documentation", [computer program] Available at: https://www.originlab.com/doc/